*Apollo 12 Preliminary Science Report*, NASA SP–235, Washington, D.C., 1970, pp. 217–223.

4. WEHNER, G. K.; AND KENKNICHT, C. E.: *Investigation of Sputtering Effects on the Moon's Surface*, NASA CR 88738, 1967.

## ACKNOWLEDGMENT

I acknowledge gratefully the helpful telephone conversations with Neil L. Nickle of the Jet Propulsion Laboratory.

# PART E

## RESULTS OF EXAMINATION OF THE RETURNED SURVEYOR 3 SAMPLES FOR PARTICULATE IMPACTS

*B. G. Cour-Palais, R. E. Flaherty, R. W. High, D. J. Kessler, D. S. McKay, and H. A. Zook*

The Meteoroid Sciences Branch at the Manned Spacecraft Center (MSC) examined the Surveyor 3 television camera housing and the length of polished aluminum tube retrieved by the Apollo 12 crew. The initial examinations were performed at the Lunar Receiving Laboratory (LRL) during a 6-day period before the return of the camera to Hughes Aircraft Co. (HAC). About 60 percent of the television camera surface area of almost 0.2 $m^2$ was scanned at 25 $\times$ magnification; each suspected impact crater on selected areas of the flat surfaces was recorded. The remainder of the camera surface was scanned at lower magnifications to insure that no significant meteoroid damage had occurred. The polished tube, 19.7 cm long and 1.27 cm wide, was scanned at a general level of 40 $\times$ magnification. Local areas of interest were examined at much higher magnifications; typical surface effects and suspected impact craters were photographed for documentary purposes.

Two 2.5-cm sections of the tube from the less uncontaminated ends, sections B and C, were examined in detail by the Meteoroid Sciences Branch after the preliminary examination at the LRL. These sections were optically scanned at 100 $\times$ magnification initially; selected areas were later examined with a scanning electron microscope. Typical samples of the polished tubing and the painted surface of the camera housing, supplied by HAC, were also examined optically to determine surface backgrounds. The meteoroid examination of the television camera showed no evidence of meteoroid damage of any consequence by primary or secondary impacts after 950 days of exposure. Five craters were found on the housing, ranging in size between 150 and 300 $\mu$m in diameter, that are thought to be characteristic of hypervelocity impact. (However, not all of these may be of meteoroid origin, as three were so closely clustered as to indicate a nonrandom origin.)

Numerous surface chips of probable low-velocity origin were observed on the television camera surface in addition to the possible meteoroid impacts. These were shallow craters generally, and primarily of recent origin, as indicated by their whiteness against the sandy-brown color of the painted surface of the television camera housing. There was a definite concentration (10 to 100 times) of these white craters on the arc of the camera housing facing the Lunar Module (LM) compared with the other side. The distribution of craters peaked at approximately a region directly in line with the LM. Protuberances on the camera such as screw heads, support struts, etc., left dark shadows of unaffected paint on the camera pointing away from the LM. The preliminary examination of the entire polished tube revealed four craters larger than 25 $\mu$m in diameter that exhibited some characteristics of hypervelocity impacts at low magnifications. Detailed examination at higher optical magnifications and with the scanning electron

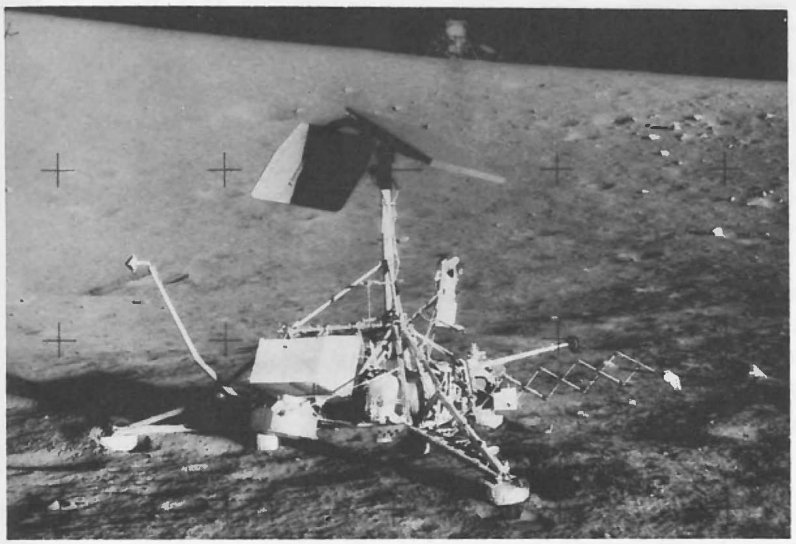

FIGURE 1.—View of the Lunar Module from the Surveyor 3 spacecraft.

microscope revealed that all of these craters were either low-velocity or polishing artifacts. The lack of meteoroid impacts of these limiting sizes is consistent with current estimates of the micrometeoroid flux on the Moon.

There is a marked concentration of pits on the same side of the tube to which a brown contamination is adhering. The material found in some of the craters is similar in composition to lunar soil.

## Location and Geometry of Landing

Apollo 12 landed about 155 m northwest of the Surveyor 3 spacecraft (ref. 1). This closeness is dramatically shown in photographs taken by the astronauts. (See fig. 1.) From such photographs, it is obvious that the LM landed on the rim of the Surveyor crater, and is approximately sitting on the horizon as seen from the Surveyor spacecraft. Note from figure 1 that the front, flat surface of the Surveyor television camera is approximately parallel to a line joining Surveyor 3 and the LM. This is also confirmed by correlating certain craters in figure 1 and those of reference 2. Such a correlation puts the LM at a camera azimuth of about 90°. Also, from reference 2, it is found that the camera is leaning toward the LM, and that the horizon, in the direction of the LM, is at a camera elevation of 25°.

The polished aluminum tube that was sectioned by the astronaut can also be seen on the Surveyor spacecraft in figure 1.

## TV Camera Housing

As previously mentioned, the camera housing was examined for evidence of meteoroid impacts during the time the camera was in the Lunar Receiving Laboratory at MSC. The time available permitted only a quick look for obvious impact craters. About 1150 $cm^2$ of the surface area was optically examined at 25 $\times$ magnification; the other surfaces were scanned at lower powers. Generally speaking, all of the flat surface areas of the housing were covered by the 25 $\times$ magnification scan; the cylindrical portions, such as the barrel and the hood, were covered at lower powers. As a result, it is correct to say that there were no damaging impacts on the camera housing. The surface of the mirror also was examined for obvious impacts.

Typical surface effects and suspected impact craters are shown in figure 2. It is interesting to note that the paint surface differs around the periphery of the housing. On the side closest to the Surveyor centerline, the surface appears grainy; on the parts facing outward, the surface is cracked like a dry river bed. Several holes and popped craters appear at the junction of cracks or along the cracks, and these were not included in the total of suspected impacts. There also was

evidence of a large number of shallow white craters covering the housing with definite concentration occurring around the periphery. The craters were obviously fresh because the original white painted surfaces had been discolored to a sandy brown and the original color was being displayed. This effect is discussed in greater detail later in this article, as the cause is probably not of meteoroid origin.

The craters identified as of possible meteoroid impact origin because of their hypervelocity also are shown in figure 2. There were five such craters ranging in size from 130 to 300 $\mu$m in diameter. However, it is likely that not all of these were caused by meteoroids. This is especially true when it is considered that three of the suspected impacts occurred on the flat mirror gear-box housing, about 25 cm$^2$ in area. If the five craters were considered to be of meteoroid origin, then the flux, allowing for lunar shielding (1/2) and spacecraft shielding (1/4), would be $1.49 \times 10^{-6}$/m$^2$/sec. Allowing for the gravitational attraction of the Earth which, at 20 km/sec, is 1.74, this is a near-Earth flux of $2.62 \times 10^{-6}$. The mass associated with the smallest crater found, 150 $\mu$m wide, is about $10^{-8.75}$ g using a crater-diameter-to-meteoroid-diameter ratio of 10. The 95 percent of upper and lower limits for five impacts is 11.7 to 1.6 according to reference 3. If this spread in flux is associated with a spread in

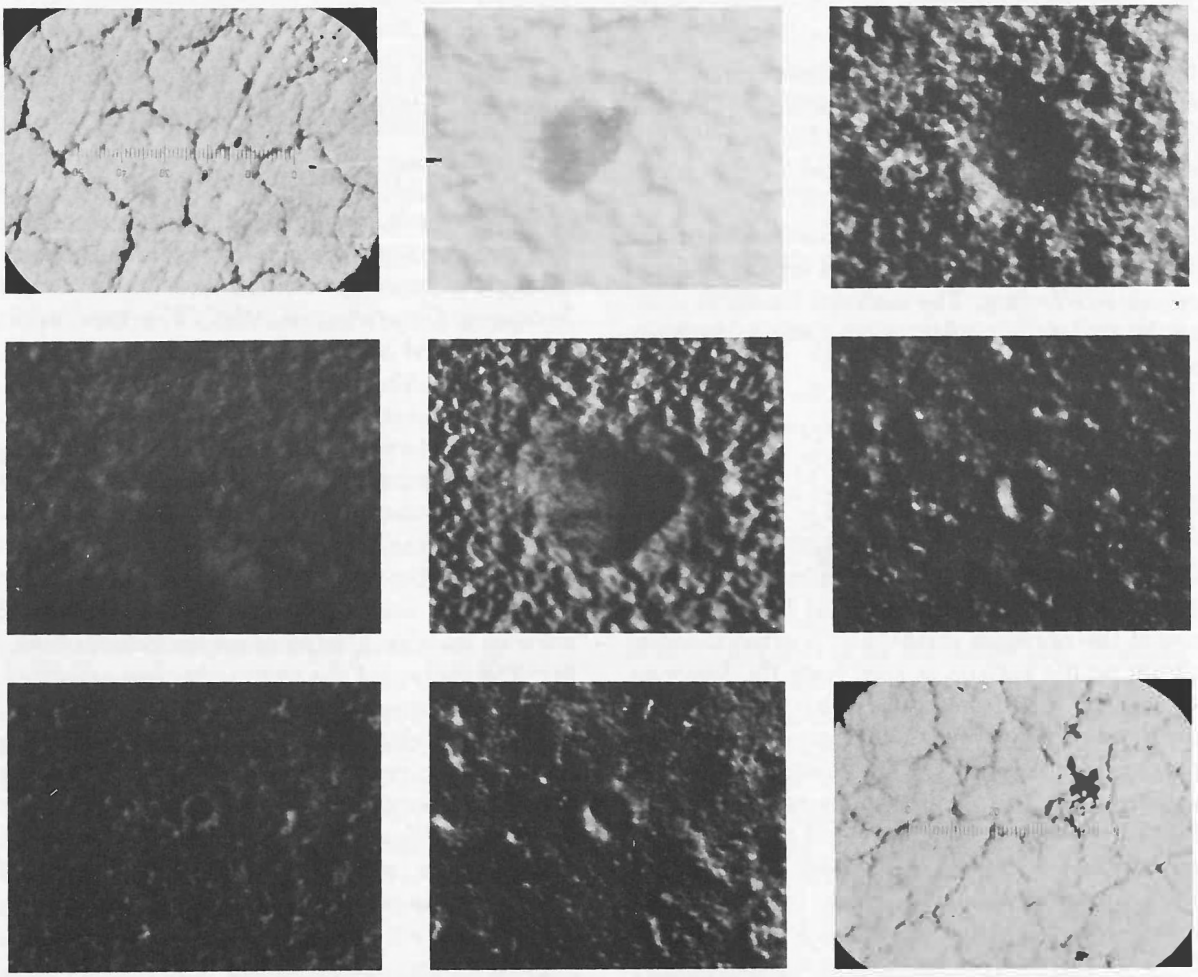

FIGURE 2.—Evidence of impacts on Surveyor 3 camera housing.

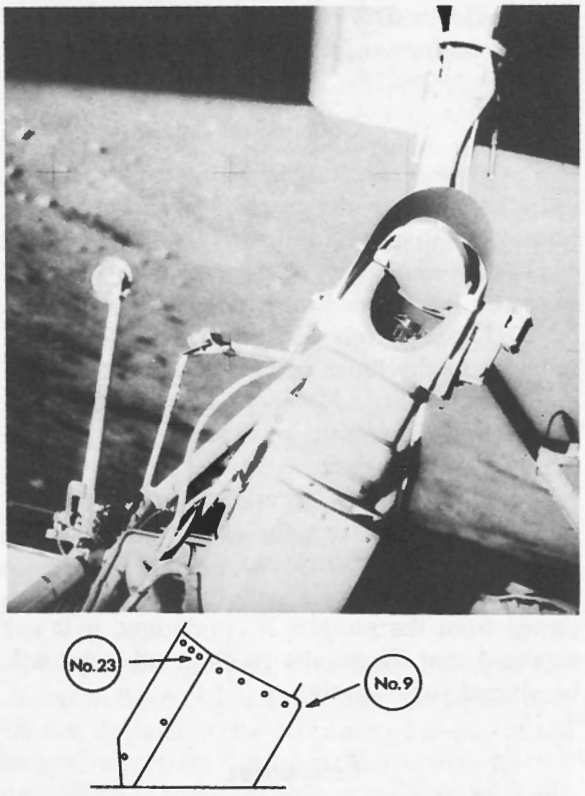


FIGURE 1.—Positions of screws 9 and 23 on the Surveyor 3 spacecraft.

tograph, screw 23 can be seen to point above the Moon's horizon at an angle of 66.6° with respect to the local upward vertical direction. Screw 9 points toward the lunar surface at the same angle with respect to the local downward vertical direction (ref. 2). Therefore, impact craters from extra-lunar particles may be expected primarily on screw 23, possibly together with low-velocity impact craters from secondary lunar debris. Screw 9 should show low-velocity impacts of secondary lunar debris.

Figure 2 shows the two screws including the washers. The investigations were made using a scanning electron microscope (Stereoscan). The scanning magnification was chosen to be 5000 ×, which allowed the identification of craters down to about 0.5 $\mu$m in diameter.

The original surfaces of the screws and washers were not specially prepared in any way for scientific investigations. They are rough and probably inadequate to yield reliable results. On screw 2 [1] (see fig. 3), strange features could be observed. Figure 4 shows six interesting objects on screw 1; these objects can be considered as impact phenomena.

The crater objects found on the screws can be compared with artificially produced micrometer-sized impact craters on metal targets. Rudolph (ref. 3) has published photographs of microcraters produced in the laboratory using a 2-MV Van de Graaff dust accelerator. Figure 5 shows some craters produced by impacts of iron projectiles on various metal targets with an impact velocity of 5.2 km/sec. The six objects on screw 1 (shown in fig. 4) appear to be low-velocity impact craters ($\leq$5 km/sec). They may have been produced either by interplanetary dust particle impacts or by secondary lunar debris from larger impacts on the lunar surface. The three objects on the surface of screw 2 (fig. 3), however, are considered to be manufacturing artifacts rather than impact craters.

[1] The identification numbers of the screws have been lost. Therefore, we have arbitrarily assigned the numbers 1 and 2 to the screws.

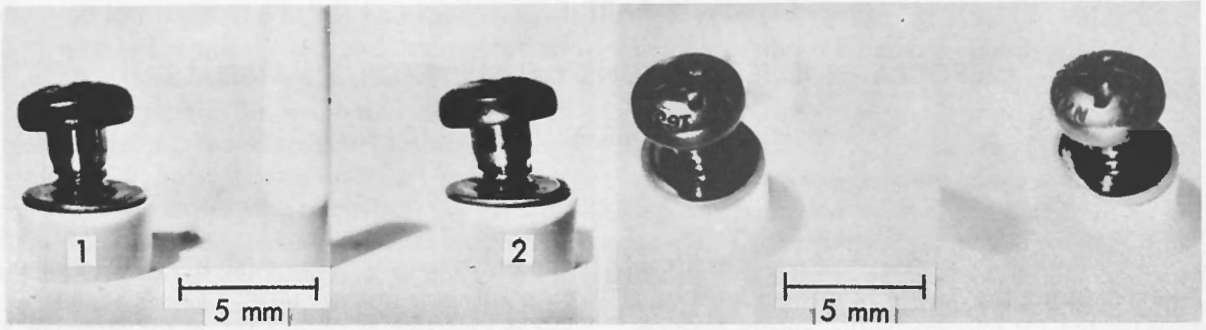


FIGURE 2.—Surveyor 3 screws with washers.

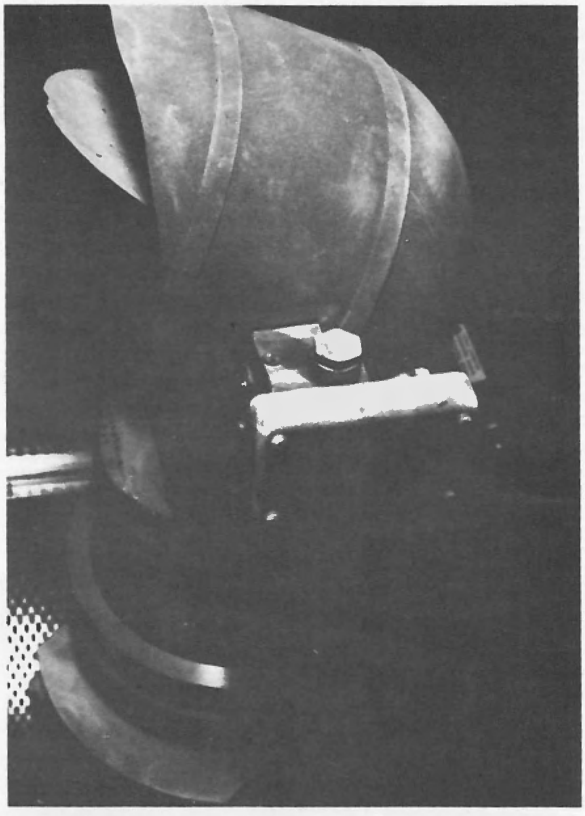

FIGURE 5.—Evidence of particle impact shadows on the camera housing.

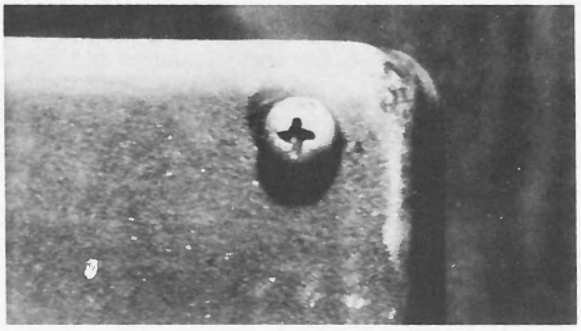

FIGURE 6.—Evidence of particle impact shadows on the camera housing.

## Polished Aluminum Tube Section

The polished aluminum tube section obtained from the Surveyor 3 spacecraft was cut from the radar altimeter and doppler velocity sensor (RADVS) support strut adjacent to leg 2 using a pair of long-handled shears (resembling pruning shears) with curved, overlapping blades. The cutting action partially flattened the ends of the tube, as may be seen in figure 9. An increase in contamination also can be seen toward the left end of the tube. This contamination appears brown to the unaided eye. Under a microscope, it also appears brown and seems to be composed, at least partially, of crystals ranging in size up to a few micrometers. As the tube is rotated, there is variation in the amount of the contamination observed.

After the tube was received at the LRL, its entire surface was scanned at a magnification of 40 × for evidence of meteoroid impact. The tube was then cut into six sections and distributed to several investigators for detailed analysis. Sections B and C, two 2.5-cm sections toward the uncontaminated end of the tube, were obtained by MSC and examined in detail for meteoritic impact evidence.

The first part of the examination was a careful optical search for impact craters performed at a magnification of 100 ×. When craters were found, optical magnifications up to 600 × were used to determine whether the craters were caused by meteoroid impact. It was expected that the very high velocities of most impacting meteoroids (averaging 15 to 20 km/sec) would leave characteristic hypervelocity impact craters which would identify them. No hypervelocity impact craters were found; however, many other craters and pits were found.

Figure 10 shows the number of craters with diameters of 20 $\mu$m and larger that were observed in the field of view of an optical microscope at 100 × magnification (corresponding to an area of about 1 mm$^2$). Counts were taken as a function of angle around the tube from the scribe line, which had been ruled along the tube before cutting. This histogram is an average of two trials on section B of the tube. Very high pit densities (up to 40 per field of view) were obtained in two places, but were obviously associated with scratches and so are not included in figure 10. The reduced count rate about 170° from the scribe line is not considered significant.

Also shown in figure 10 is a measure of the relative amounts of brown contamination on section B as a function of angle around the tube. This curve was obtained by photographing the

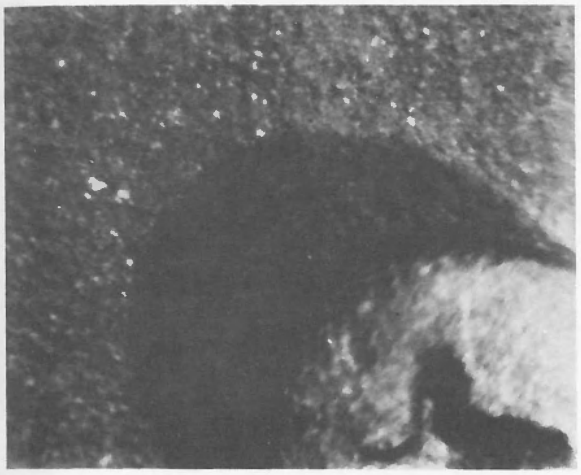

FIGURE 7.—Evidence of particle impact shadows on the camera housing.

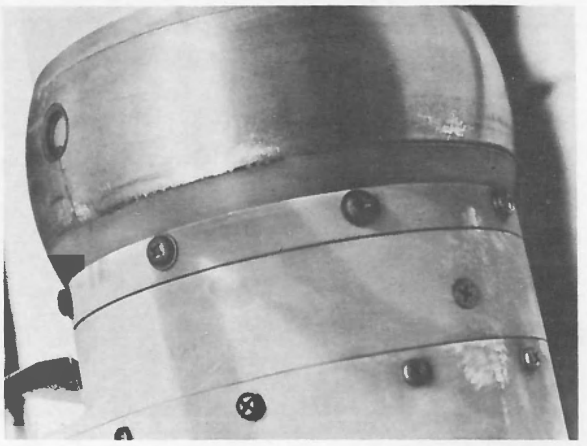

FIGURE 8.—Shadows of the attachments on the television camera housing.

tube at each angular position, as the tube was rotated and the lighting held constant. The contamination stood out in the photographs between the angles of 100° and 280° and seemed to peak at about 190°. Outside of these angles, section B was relatively clean. The relative heights of the ordinate of the contamination curve in figure 10 are not quantitatively significant. A high ordinate means that the photograph indicates "high" contamination relative to an angular position with a ordinate. It is immediately evident that there is a close association between the pitting rate and density of the brown contamination.

In addition to the optical work, extensive analyses were performed using a scanning electron microscope (SEM). The SEM was used in three modes of analysis:

(1) To look at higher magnifications of craters found during the optical scan of tube sections B and C in order to determine the origin of these craters.

(2) To perform a spot survey at high magnifications over all of section C.

(3) To determine, by non-dispersive X-ray analysis, the composition of material in the craters and on the surface of the tube.

The results were—

(1) No craters showed evidence of hypervelocity impact origin. (It was not possible, by optical methods alone, to determine whether or not some of the smaller craters had hypervelocity im-

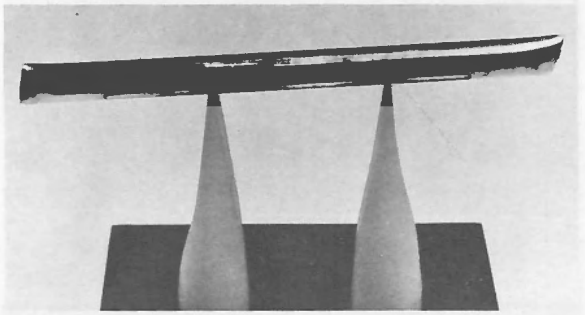

FIGURE 9.—Polished aluminum tube section obtained from the Surveyor.

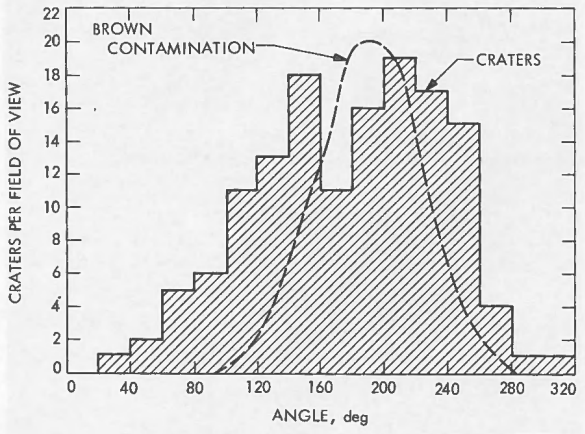


FIGURE 10.—Distribution of brown contamination and of impact craters.

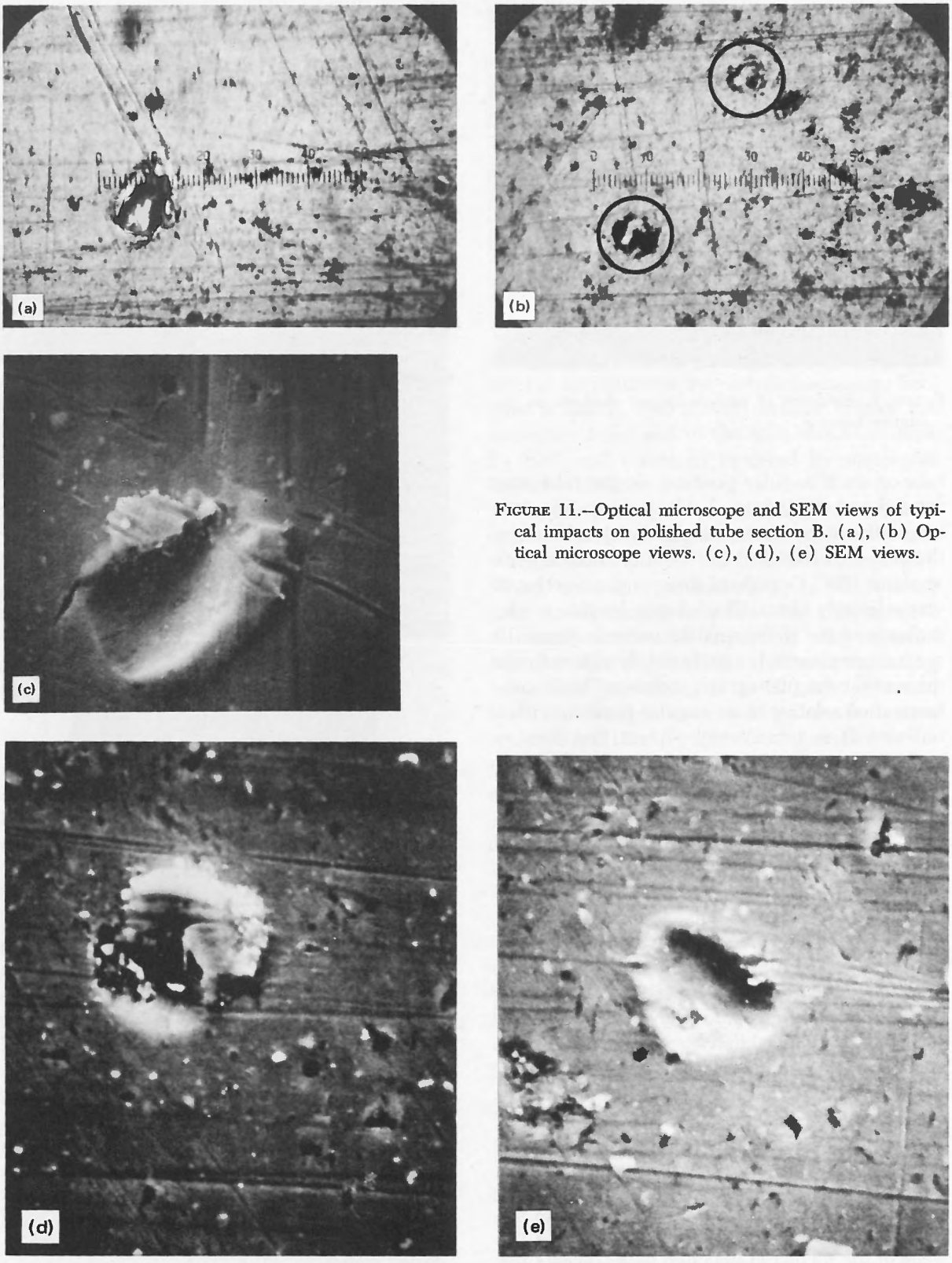


FIGURE 11.—Optical microscope and SEM views of typical impacts on polished tube section B. (a), (b) Optical microscope views. (c), (d), (e) SEM views.

pact characteristics.) On the contrary, all of the craters examined appeared to have a low-velocity impact origin and many of them had material remaining in them.

(2) The spot survey of section C confirmed the pitting density results of the optical scans, but added little new information.

(3) Analysis of the material in the craters strongly indicated that most of it was of lunar origin.

The brown contamination on the surface did not give any peaks because elements with X-ray energies below about 1 kV are not detectable with the analyzer on this SEM. Thus, elements such as oxygen, nitrogen, carbon, etc., would not have been discovered in this analysis.

Figure 11 shows SEM photographs of three craters on section B, located 280° from the scribe line. The craters obviously are not due to a hypervelocity impact; e.g., there is no smooth, raised lip entirely around the central indentation. However, it is clear that material at relatively low velocity, perhaps a few hundred meters per second, has impacted from the lower left in this photograph. The largest crater is about 30 $\mu$m wide, and material is still in the crater. An X-ray pulse height analysis of this material showed it to be composed of silicon, calcium, and iron with significant traces of chromium and titanium.

Figure 12 shows a region of high pitting density at 220° from the scribe line on section B. The

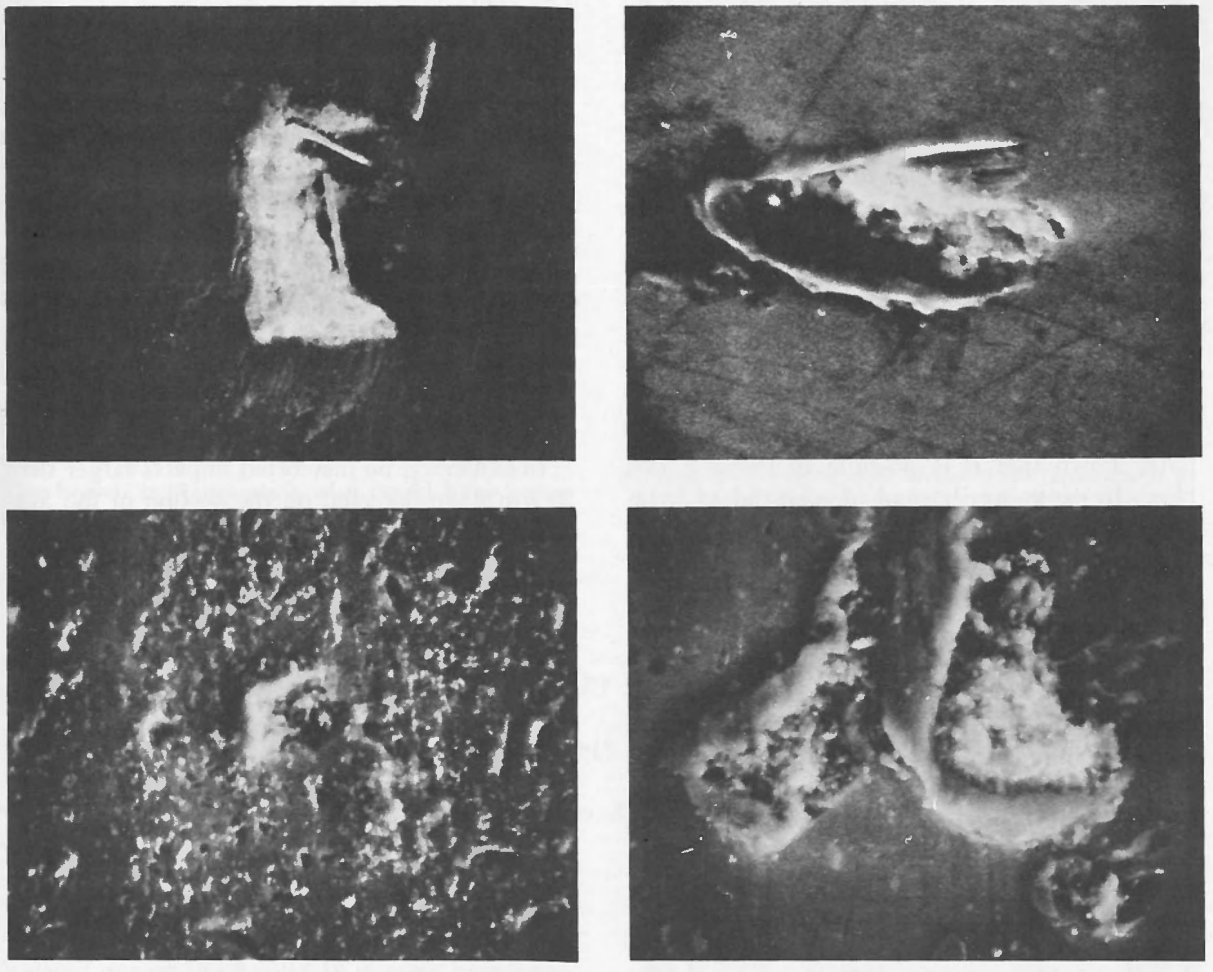

FIGURE 12.—Evidence of typical impact debris found on sections B and C of the Surveyor 3 polished tube.

crater in the center is about 8 $\mu$m in diameter; the material in this crater has as major components silicon, iron, calcium, and titanium. Titanium was also found in another crater on this tube. Because only six craters were extensively analyzed by SEM non-dispersive X-ray analysis, the significant amounts of titanium found in three of them are indicative of a lunar origin. From the mineralogical standpoint, at least three phases are present:

(1) A calcium aluminum silicate, which is undoubtedly plagioclase.

(2) A calcium iron magnesium silicate with a trace of titanium, which is consistent with clinopyroxene.

(3) One containing calcium, iron, titanium, and silicon in varying amounts and possibly also containing aluminum and magnesium. This is probably glass and unresolvable mixtures of very fine fragments.

A crater that gave us some difficulty is the one shown in figure 12 at 170° from the scribe line. Its size is about 80 by 110 $\mu$m and is one of the largest craters on the tube. The reason for the difficulty was the surprising appearance of "rods" in the crater, which looked very much like glass fibers under an optical microscope. The SEM analysis showed them to be identical in composition to the glass fibers in the astronauts' outer garments and in the back pack in which the Surveyor 3 parts were stowed. Experiments at MSC have shown that it is possible to break a few fibers by jamming the end of a strand of beta-fiber into a crater of this size.

As no meteoroid impacts were found on the tube, it is possible to set upper limits to the meteoroid flux at the Moon. The detection threshold over the entire tube corresponds to craters about 50 $\mu$m wide. The highly contaminated region was sufficiently pitted and scarred as to make it impracticable to resolve features of smaller craters. On the non-pitted sides of sections B and C, the detection threshold corresponds to 25 $\mu$m and larger craters. The effective non-pitted region is about one-half the area of these sections. If it is assumed that meteoroid impact craters are hemispherical in shape, then the threshold penetration depths are, respectively, 25 $\mu$m over the entire tube and 12.5 $\mu$m over one-half each of two 2.5-cm sections.

The 50-$\mu$m threshold over the entire tube corresponds to a meteoroid 14.5 $\mu$m wide and with a mass of $10^{-8.8}$ g. The 25-$\mu$m threshold corresponds to a meteoroid 7.5 $\mu$m in diameter and $10^{-9.66}$ g in mass. These masses correspond to a 20-km/sec impact velocity and a 1-g/cm density. The area of the entire tube is about 78.5 cm$^2$; the area of the non-pitted regions of sections B and C is 10.1 cm$^2$. If it is appropriate to use a shielding factor of one-half due to Moon and another factor of two-thirds due to the fact that the Surveyor spacecraft obliterates about one-third of the remaining solid angle from which meteoroids could approach, the effective area-time exposures are $2.16 \times 10^5$ m$^2$ sec for the entire tube and $2.8 \times 10^4$ m$^2$ sec for the non-pitted regions of sections B and C. Upper confidence limits of 95 percent on the meteoroid flux for no impacts for area-time exposures of $2.16 \times 10^5$ m$^2$ sec and $2.8 \times 10^4$ m$^2$ sec are, respectively, $10^{-4.75}$ impacts/m$^2$/sec and $10^{-3.88}$ impacts/m$^2$/sec. To compare these upper limits of the Moon with fluxes of Earth, one must allow for a gravitational flux increase factor of 1.74 at the Earth. Hence, the corresponding upper limits at Earth would be $10^{-4.51}$ impacts/m$^2$/sec for masses larger than $10^{-5.8}$ g and $10^{-3.64}$ impacts/m$^2$/sec for masses larger than $10^{-9.66}$ g. These upper limits are in good agreement with penetration measurements but not with older acoustic measurements, as can be seen in figure 3.

In summary, no meteoroid impacts larger than 25 $\mu$m were detected on the section of the Surveyor 3 strut returned from the Moon. The close association between the brown contamination and the pits on this section is significant. Also, the fact that there is lunar material in the pits is evidence that this phenomenon occurred while the Surveyor 3 spacecraft was on the Moon. Three possibilities for an origin to the pitting and contamination are—

(1) Lunar secondary and tertiary ejecta disturbed by primary meteoroid impacts bombard the exposed area of the tube, causing the pitting. The contamination is also composed of lunar material. The evidence from the sheared ends of the tube, however, has the contaminated and pitted side of the tube pointing away from a direction from which secondary ejecta is likely to approach. SEM analysis of the contamination

was unable to show any elements with atomic numbers greater than 11 (sodium); thus, it is unlikely that the brown contamination is composed of lunar soil.

(2) The pitting is due to lunar material blasted toward the Surveyor 3 spacecraft by the Apollo 12 LM as it landed. This possibility cannot be discounted, as has been shown previously for the camera housing. Experiments have shown that parts of the tube are visible from the LM. Two problems arise with this hypothesis. One is that the pitting on the tube seems to be more intense than on the camera; the other is that the camera seems to have been brown before the LM landed (and in a somewhat uniform fashion). However, the pitted side of the tube was darkened.

(3) The pitting is due to lunar material blasted toward the tube by the vernier engines; the contamination is due to incompletely burned propellant (unsymmetrical dimethyl hydrazine monohydrate fuel combined with nitrogen tetroxide oxidizer, with some nitrous oxide added as a catalyst). This also is a possible source, as the contaminated side of the tube could point down toward the lunar surface and somewhat in toward the Surveyor spacecraft if the tube is rotated 180° about the astronaut's cutter axis relative to possibility (2).

The Surveyor strut seems to have been pitted by lunar material disturbed by either the LM descent stage or the Surveyor 3 vernier engines. The brown contamination also could have come from either source, as the propellants used are nearly identical. We feel that the Surveyor 3 vernier engines are the more logical source.

## Conclusions

The general conclusions arising from the MSC examination of the Surveyor 3 television camera housing and polished tube are—

(1) Meteoroid flux at the lunar surface is as expected from near-Earth measurements.

(2) Lunar ejecta flux related to meteoroid impacts on the lunar surface could not be specifically identified. However, other non-natural sources of low-velocity impacts by lunar surface material were evident.

(3) Lunar surface experiments and hardware must be shielded from the effects of spacecraft jet-exhaust-induced impacts.

Although additional analysis of the data obtained from the samples is continuing, it is not expected that the results given at this time will be altered significantly.

## References

1. *Apollo 12 Preliminary Science Report,* NASA SP–235, Washington, D.C., 1970.
2. *Surveyor III—A Preliminary Report,* NASA SP–146, Washington, D.C., 1967.
3. RICKER, W. E.: "The Concept of Confidence or Fiducial Limits Applied to the Poisson Frequency Distribution." *Journal of the American Statistical Association,* vol. 32, 1937, pp. 349–356.
4. *Meteoroid Environment Model–1969 (Near Earth to Lunar Surface),* NASA SP–8013, Washington, D.C., 1969.

# PART F

# MICROCRATER INVESTIGATIONS ON SURVEYOR 3 MATERIAL

*E. Schneider, G. Neukum, A. Mehl, and H. Fechtig*

Two screws from the Surveyor 3 spacecraft recovered during the Apollo 12 mission have been investigated for micrometeorite impact features. A general description of the scientific investigations of Surveyor 3 material is given in reference 1.

The positions of the screws on the Surveyor 3 spacecraft are shown in figure 1. From this pho-